Overcoming status quo bias in the human brain

Stephen M. Fleming[a,1], Charlotte L. Thomas[a,b], and Raymond J. Dolan[a]

[a]Wellcome Trust Centre for Neuroimaging, University College London, London WC1N 3BG, United Kingdom; and [b]Faculty of Medicine and Dentistry, University of Bristol, Bristol BS2 8DZ, United Kingdom

Edited by Robert Desimone, Massachusetts Institute of Technology, and approved February 16, 2010 (received for review September 11, 2009)

Humans often accept the status quo when faced with conflicting choice alternatives. However, it is unknown how neural pathways connecting cognition with action modulate this status quo acceptance. Here we developed a visual detection task in which subjects tended to favor the default when making difficult, but not easy, decisions. This bias was suboptimal in that more errors were made when the default was accepted. A selective increase in subthalamic nucleus (STN) activity was found when the status quo was rejected in the face of heightened decision difficulty. Analysis of effective connectivity showed that inferior frontal cortex, a region more active for difficult decisions, exerted an enhanced modulatory influence on the STN during switches away from the status quo. These data suggest that the neural circuits required to initiate controlled, nondefault actions are similar to those previously shown to mediate outright response suppression. We conclude that specific prefrontal-basal ganglia dynamics are involved in rejecting the default, a mechanism that may be important in a range of difficult choice scenarios.

decision making | functional MRI | subthalamic nucleus | action | conflict

When faced with a complex decision, people tend to accept the status quo, as reflected in the old adage, "When in doubt, do nothing." Indeed, across a range of everyday decisions, such as whether to move house or trade in a car, or even whether to flip the TV channel, there is a considerable tendency to maintain the status quo and refrain from acting (1). One factor driving this status quo bias is the difficulty of the decision process. In supermarkets, for example, there is often an overwhelming choice of different brands for the same product, and consumers may leave the store empty handed because of a difficulty-induced bias toward inaction (2, 3).

Here we shed light on the brain mechanisms involved in making difficult decisions involving a status quo. We operationally define a status quo bias as suboptimal acceptance of a default choice option (Fig. 1*B*). The neural mechanisms involved in overcoming this bias are unknown, but informative parallels can be derived from the effects of treatments for Parkinson's disease. Akinesia, a core symptom of Parkinson's, can be alleviated by disruption of the basal ganglia either by neurosurgical lesions or deep-brain stimulation (DBS) (4, 5). Despite these beneficial therapeutic effects, it is known that DBS of the subthalamic nucleus (STN) in Parkinson's patients can lead to impairments of cognitive control (6–8), suggesting that one of the core functions of the STN is to modulate basal ganglia circuits involved in decision making (9–11). An anatomic "hyperdirect" pathway from medial and lateral prefrontal cortex, previously characterized in primates (12) and humans (13), may mediate cognitive influences on the STN (14–16). Here we tested whether interactions between the frontal cortex and basal ganglia provide candidate mechanisms for how decision difficulty modulates choices involving a status quo.

We asked participants to make sensory judgments in the context of a tennis "line-judgment" game (Fig. 1*A*) while undergoing functional MRI (fMRI). We selected this game on the basis of its natural default option—line judges remain silent to indicate that the ball was "in," but make an overt response by shouting "out" to reject the default. Further, such a task involves graded perceptual difficulty (17). A status quo bias in this task can be modeled by assuming that a decision criterion is biased depending on whether the default is set to "IN" or "OUT" (Fig. 1*B*). The qualitative prediction from this model is that when the decision is difficult, a criterion shift has more impact than when the decision is easy (Fig. 1*B*, *Bottom*), leading to a status quo bias on high- but not low-difficulty trials (see Fig. 1 legend for further details of the model). To examine brain mechanisms for overcoming this bias, we implemented a simple factorial design by crossing high and low decision difficulty with rejection or acceptance of the default. Conceptually similar approaches have been used in animal experiments to decouple the neural processing related to response execution from that associated with variables affecting the decision (18).

The status quo bias can be shaped by a number of complex and interacting factors, such as the economic costs involved in making the transition (1, 19), aversion to losing what one presently owns (20, 21), and the potential for regretting a change (22). Here we restrict our investigation to the ubiquitous factor of decision difficulty, minimizing the influence of other, potentially confounding psychological variables. In our simple visual detection task, the choice set size remains constant (two-alternative forced-choice), and outcomes are omitted, allowing examination of the neural integration of decision difficulty with acceptance or rejection of the status quo.

Results

Behavior. In line with theoretical predictions (Fig. 1*B*), there was a greater tendency to accept the default on high- compared with low-difficulty trials [$t(15) = 2.51, P < 0.05$; Fig. 2*A*]. This bias toward default acceptance was seen in 13 of 16 subjects and importantly resulted in suboptimal choice behavior. There was an increase in errors when accepting (compared with rejecting) the default on high- but not low-difficulty trials, leading to an interaction of difficulty and response type [$F_{(1,15)} = 6.09, P < 0.05$]. Post hoc paired t tests confirmed that this interaction was driven by a significant increase in error rates when the default was accepted on high-difficulty trials relative to when it was rejected [$t(15) = 2.45, P < 0.05$], with no differences in low-difficulty default acceptance and rejection errors [$t(15) = 0.58, P = 0.57$]. These behavioral effects were replicated in a separate experiment ($n = 18$) outside the scanner (Fig. S1).

Judgement accuracy on low-difficulty trials was 95.1% ± 1.0% (SEM). By design, accuracy on high-difficulty trials was reliably lower [$t(15) = 24.3, P < 0.0001$] but remained significantly above chance [58.0% ± 1.3% SEM, one-sample t test against 50%, $t(15) = 5.71, P < 0.001$]. As expected, rejection reaction times (RTs) were greater on high- compared with low-difficulty trials [$t(15) = 5.28, P < 0.001$]. The distribution of RTs in the two difficulty conditions is shown in Fig. 2*B*.

We next computed signal detection theory (SDT) measures from our data by classifying trials according to the model pre-

Author contributions: S.M.F., C.L.T., and R.J.D. designed research; S.M.F. and C.L.T. performed research; S.M.F. analyzed data; and S.M.F. and R.J.D. wrote the paper.

The authors declare no conflict of interest.

This article is a PNAS Direct Submission.

Freely available online through the PNAS open access option.

[1]To whom correspondence should be addressed. E-mail: s.fleming@fil.ion.ucl.ac.uk.

This article contains supporting information online at www.pnas.org/cgi/content/full/0910380107/DCSupplemental.

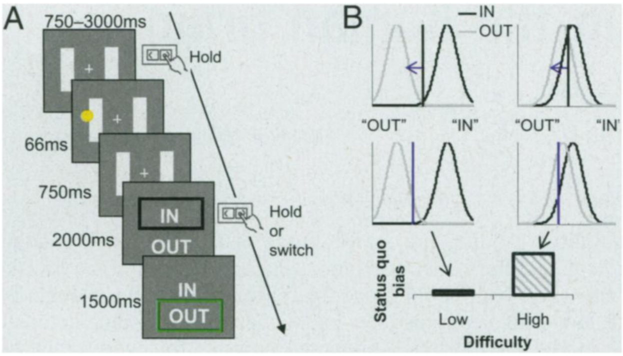

Fig. 1. Task design. (*A*) Participants played a "tennis line-judgment" game in which the default was systematically manipulated in a balanced factorial design. At the beginning of each trial, participants were asked to depress the "default" key and fixate on the cross between the two tramlines. They then saw a ball land on the court, before being asked to make a decision on whether it was "IN" (overlapping the line) or "OUT." This decision was indicated by continuing to depress the key to accept the default, or releasing it and switching to the opposite key to reject. Easy and difficult (low and high difficulty) trials were randomly interleaved within a block and balanced across whether the correct response was to accept or reject the default. (*B*) A possible theoretical account of the status quo bias in our task. We assume that the appearance of the ball gives rise to an internal state along an arbitrary decision axis sampled from separate IN (black) and OUT (gray) probability distributions. These probability distributions are nonoverlapping for low-difficulty decisions (*Left*) but overlap considerably for high-difficulty decisions (*Right*). The vertical line in each case represents the decision criterion—how the observer splices up this decision axis to report IN or OUT. The upper row shows an ideal observer's neutral criterion (black line), the lower row a criterion biased toward the accepting the default (blue line; here, reporting "IN"). A shifted criterion has more impact on stimuli drawn from overlapping probability distributions, leading to a greater status quo bias on high-difficulty trials.

sented in Fig. 1*B* (*Methods*). This analysis confirmed shifts in criteria (c) as a function of default position (in/out) on high-difficulty trials ($c_{\mathrm{in}} = 0.31$, $c_{\mathrm{out}} = -0.48$) but not low-difficulty trials ($c_{\mathrm{in}} = 0.049$, $c_{\mathrm{out}} = 0.0052$), leading to a significant interaction of default and difficulty level [$F_{(1,15)} = 9.84$, $P < 0.01$]. Changes in sensitivity (d') due to difficulty level did not interact with default position [in/out;'$F_{(1,15)} < 1$, $P = 0.69$].

fMRI Analysis. Our behavioral findings of a status quo bias for high- but not low-difficulty trials motivated us to explore the neural basis of this interaction. Crucially, we were interested in regions showing differential activity for rejection of the status quo under high but not low difficulty. To isolate such regions, we computed an interaction contrast [*reject_high* – *accept_high*] – [*reject_low* – *accept_low*]. In this interaction we found activation in right STN region that survived correction for the whole brain [$P < 0.05$, family-wise error (FWE) corrected; Fig. 3*A*; see *SI Text* and Fig. S2 for anatomic localization). Similar activation was found in left STN region [$P < 0.05$, small-volume corrected (SVC); Fig. 3*A*]. No other brain regions survived whole-brain correction, and the reverse contrast did not reveal any other significant interaction effects. To further explore the observed interaction, we computed percentage signal change for each trial type, averaging over all voxels within anatomically defined STN regions of interest (ROIs) (11) and entered these values into a repeated-measures ANOVA [factors *STN_side* (left/right) × *decision* (accept/reject) × *difficulty* (high/low)]. We confirmed a significant interaction between decision difficulty and default rejection [$F_{(1,15)} = 17.70$, $P < 0.001$] that was consistent across both left and right STN [no three-way interaction with *STN_side*; $F_{(1,15)} < 1$, $P = 0.80$]. A main effect of *decision* was also present [greater activity on reject trials; $F_{(1,15)} = 18.04$, $P < 0.001$].

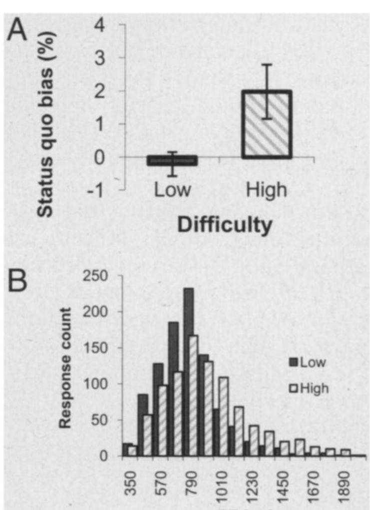

Fig. 2. Behavioral results. (*A*) Status quo bias was calculated as the percentage of default acceptance greater than 50% on both high- and low-difficulty trials. A bias toward accepting the default was seen on high- but not low-difficulty trials, resulting in suboptimal choice behavior. This pattern of results was replicated in an independent sample outside of the scanner (Fig. S1). Error bars reflect ±SEM. (*B*) Histogram of RT counts across subjects for high- and low-difficulty rejection responses, showing slower (more negatively skewed) RTs on high-difficulty trials.

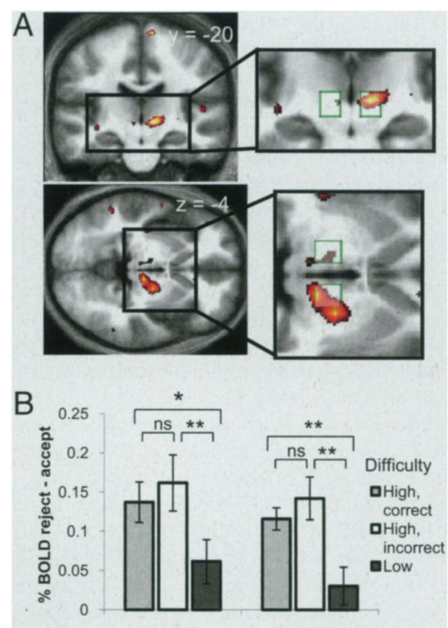

Fig. 3. Interaction of decision difficulty and default rejection. (*A*) T-map for the interaction contrast [(*reject_high* – *accept_high*) – (*reject_low* – *accept_low*)], shown in coronal and axial sections (*Right:* $P < 0.05$, whole-brain corrected; *Left:* $P < 0.05$, SVC; shown at $P < 0.005$, uncorrected). Activity is seen bilaterally in the region of the STN (peak voxels; *Left:* −6, −24, −3; *Right:* 12, −18, 0). *Insets:* Overlap between the active clusters and STN ROIs (10 × 10 × 10-mm boxes centered on ±10, −15, −5). (*B*) Average difference in percentage signal change (*reject* – *accept*) calculated from an unbiased average of all voxels within each STN box ROI. Events are split as a function of difficulty level. High-difficulty trials were further split into correct and incorrect (the relative rarity of an incorrect, low-difficulty response precluded the same split on low-difficulty trials). The interaction effect was driven by a greater STN response for rejecting the default on high- compared with low-difficulty trials. Post hoc paired *t* tests: *$P < 0.05$, **$P < 0.005$. Error bars reflect ±SEM.

Specifically, the interaction effect is driven by increases in STN activity on trials in which the default is rejected in the face of high decision difficulty, as shown in Fig. 3*B*. This difference is similar for both correct and incorrect responses (no difference between gray and white bars in Fig. 3*B*), suggesting that the behavioral difference in accuracy for *accept_high* and *reject_high* responses cannot explain the signal change we observe in the STN.

As expected, we found a widespread motor network (Table S1) when contrasting *reject* > *accept* responses, with greater activity on the left side consistent with rejection responses being made with the contralateral (right) hand. The reverse contrast, *accept* > *reject*, did not reveal any significant activations. Contrasting both trial types against baseline revealed activity in the pre–supplementary motor area that was common to both decision types (Fig. S3 and *SI Text*). Activity in bilateral inferior frontal cortex (IFC; $P < 0.05$, FWE whole-brain corrected) and bilateral medial frontal cortex (MFC; both $P < 0.05$, SVC) correlated with increasing RT for rejecting the default (Fig. 4*A* and Table S2). We saw additional main effects of decision difficulty in both MFC ($P < 0.05$, FWE whole-brain corrected) and IFC ($P < 0.001$, uncorrected) (Table S3), in line with specific recruitment of these regions during situations requiring increased cognitive control (10, 15). The parametric correlation with RT did not interact with difficulty level ($P > 0.005$, uncorrected), suggesting that our low-difficulty condition may still have induced some degree of adaptive slowing (cf. ref. 10). Other regions activated in these contrasts are detailed in Tables S2 and S3.

Modeling Neural Interactions During Status Quo Rejection. We hypothesized that the signal observed in the STN may reflect an integration of inputs from frontal cortical regions sensitive to decision difficulty, making status quo acceptance less likely. We therefore tested a connectivity model (dynamic causal model; DCM) derived from theoretical models of action selection (8, 9, 23) in which both MFC and IFC, anatomically connected with the STN region in humans (13), were hypothesized as providing biasing influences. Building on the known role of right IFC (rIFC) in cognitive control (14) and the robust interaction effect we see in right STN, we restrict our DCM analysis to the right hemisphere (Table S4). Our primary aim was to establish how trial-by-trial decision difficulty and the likelihood of default rejection influence information flow in this circuit, thus constituting a possible mechanistic explanation for the interaction effect seen in the STN (24). More specifically, we asked whether default rejection is reflected in a modulation of connection strength from rIFC to STN, from MFC to STN, or both.

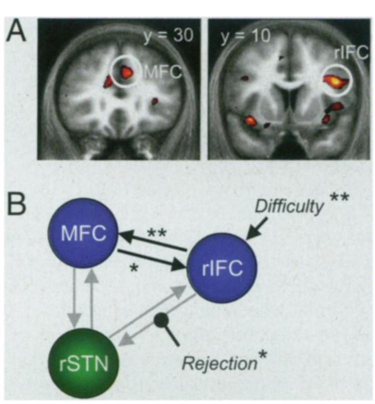

Fig. 4. Effects of decision difficulty and default rejection on connectivity. (*A*) Coronal sections are shown through the group T-map for positive correlations with the RT regressor (shown at $P < 0.005$, uncorrected). Circled are the regions that were entered into the subsequent connectivity analysis. (*B*) Schematic showing the winning DCM model and the pattern of significant connections. Default rejection (*reject*) was associated with increased influence of the rIFC on the STN. *$P < 0.05$, **$P < 0.005$.

In DCM, the statistical likelihood that an evoked response is driven by activity in another brain area is modeled by a set of coupled bilinear differential equations (25), resting on a generative model of underlying neural activity. In our model, the modulatory influence of default rejection (*reject*) was inferred from the responses of the subject on any given trial, and is taken to reflect the intentional "hidden" state of the decision maker during the choice period. A driving input to frontal cortical areas was provided by a variable encoding trial-by-trial difficulty (*high* = 1, *low* = 0), which could enter into either rIFC, MFC, or both. Bayesian model comparison revealed the class of models with difficulty entering into the network via the rIFC to be superior to other considered model classes (Fig. S4; combined exceedence probability of 87.9%). Within this class of models, models 5 and 6 had similar exceedence probabilities, with model 6 differing from model 5 by a single extra parameter (*reject* modulating MFC to STN, which did not reach group-level significance). We focus on the simplest winning model 5 shown in Fig. 4*B*, while noting that results from model 6 (reported in Table S5 and *SI Text*) support similar conclusions.

Crucially, connectivity was systematically increased from rIFC to STN when subjects rejected the default [$0.06\ s^{-1}$, $t(13) = 2.43$, $P < 0.05$]. Baseline (endogenous) connectivity from rIFC to STN was on average positive (mean = $0.04\ s^{-1}$), but was not significant in the absence of default-related modulation ($P = 0.34$). Because modulatory parameters (in this case, the influence of default rejection) in DCM are expressed as fractions of baseline connectivity, we infer that default rejection invokes prefrontal–STN dynamics that are largely absent when the status quo is accepted. Baseline connectivity was consistently positive from rIFC to MFC [$0.17\ s^{-1}$, $t(13) = 4.11$, $P < 0.005$] and from MFC to rIFC [$0.02\ s^{-1}$, $t(13) = 2.68$, $P < 0.05$] and was significantly greater from rIFC to MFC than in the reverse direction [$t(13) = 4.25$, $P < 0.001$]. Decision difficulty was a significant driver of rIFC [$0.03\ s^{-1}$, $t(13) = 3.53$, $P < 0.005$]. To summarize, our DCM results are consistent with a robustly increased drive from rIFC to STN when the default is rejected in the face of increased decision difficulty.

Discussion

Our results show that participants are more likely to accept the status quo when faced with difficult choices, leading to more errors. This suboptimal choice behavior implies that the status quo bias may disconnect people's preferences from their subsequent choices. For example, employees often accept a company's default retirement plan even if it leads to poorer investments (26). Similarly, consumers become impassive in the face of overwhelming choice, leading to a fall in the number of purchases (3). Common to both these scenarios is a difficult decision and the opportunity to remain with the status quo.

Our brain imaging findings provide a neural basis for how such a status quo bias might be overcome. In our fMRI data, rejection of the default on difficult trials recruited bilateral regions encompassing the STN, a component of the basal ganglia thought to play a pivotal role in action selection (5, 9). Specifically, blood oxygen level–dependent (BOLD) signal increased in both left and right STN when the default was rejected on difficult, but not easy, trials. This effect was not explained by a change in decision accuracy. Instead, the interaction suggests a specific role for STN activity in overcoming a status quo bias induced by increasing choice difficulty.

Our connectivity model further provides a possible mechanistic explanation both for the difficulty-induced bias toward the status quo shown in Fig. 2*A* and the pattern of STN signal change shown in Fig. 3*B*. On easy trials, a bias favoring inaction may not need to be militated against to maintain accurate decisions (Fig. 1*B*, *Left*). In contrast, on difficult trials, this same bias leads to suboptimal acceptance of the default (Fig. 1*B*, *Right*, and Fig. 2*A*). We suggest

NEUROSCIENCE

PSYCHOLOGICAL AND COGNITIVE SCIENCES

that increased drive from rIFC to the STN under conditions of high difficulty is causal in tempering this bias (making decision criteria more "neutral" under high-difficulty conditions; Fig. 1*B*). This context-dependence of STN activity is consistent with findings from DBS studies that report a role for the STN under conditions of high but not low difficulty (6–8). An alternative account might suggest that the activation we observe is epiphenomenal, rather than being causal in the amelioration of a status quo bias. We consider this possibility as less likely, for a number of reasons. First, the activity increase observed is specific to rejecting a difficult default, rather than rejection of the default per se, and is not easily explained through simple correlation with motor output or decision accuracy. Second, the effects we observe are consistent across bilateral STN, a region proposed as a key node for control of decision making (9, 10). Finally, and perhaps most persuasively, DBS in Parkinson's disease reveals a causal role for the STN in the modulation of decision making (6–8, 27, 28), and lesions to the STN in rodents produce impaired response selection under situations of high conflict (29, 30).

The pattern of activity in the STN region can be further examined in the context of two influential models that address the broader role of the basal ganglia in decision making (9, 10). In brief, it is proposed that activation of striatal neural populations by salient sensory stimuli drives selection of an appropriate response, releasing the pallidal inhibition of the thalamus. A "hyperdirect" pathway from frontal cortex to the STN (12) leads to modulation of pallidal–thalamic responses as a result of decision difficulty (9), adjusting basal ganglia output. In support of a hyperdirect modulation of STN activity, we find that an inferior frontal region sensitive to task difficulty drives the STN in our DCM. Within our task and model constraints default-related modulation of the STN was best explained by a pathway from rIFC, consistent with a direct white matter tract linking these regions (12, 13). However, we anticipate a contribution of the MFC to STN modulation in other scenarios, such as outright response inhibition (see below) and note data suggesting influences of midline EEG potentials on STN responses (31, 32). In addition, both IFC and MFC activity may affect default rejection in our task via pathways that bypass the basal ganglia, consistent with short-latency modulation of primary motor responses after stimulation of these structures (33, 34).

Studies of the stop-signal RT task using fMRI have isolated both the rIFC and STN as critical nodes in stopping of responses (11, 35, 36). Disrupting rIFC with transcranial magnetic stimulation leads to failure of response inhibition (37), and individual differences in rIFC volume predict successful stopping (38). Similarly, DBS of the STN in patients with Parkinson's disease directly modulates stop-signal RTs (27, 28). In our task, a simple inhibitory account of STN function would suggest greater activity when a difficult default is accepted (lack of action), whereas an account that emphasizes a role for the STN in controlled responding would predict greater activity when the default is rejected. Our data favor the latter view, and together with related evidence (13, 16) implicate the STN in both outright response suppression and controlled slowing or switching. Indeed, the acceptance or rejection of a prepotent response may be orthogonal to the action-inhibition distinction. In some situations the default is to respond and the controlled response is to inhibit, whereas in others (such as when judging the line in tennis), the default is to remain silent, and the controlled response is to initiate an overt action (39). This hypothetical dissociation raises intriguing and testable hypotheses for further interventional research: if the dominant function of the STN is to inhibit action, then lesions or electrical disruption in a task such as ours should result in a tendency to respond, and a decreased status quo bias. However, if its dominant function is to initiate a controlled mode of responding, STN dysfunction would lead to an increased status quo bias.

In summary, we describe a neural mechanism for overcoming a difficulty-induced status quo bias centered on IFC/STN. We show that difficult choice scenarios lead to greater acceptance of the status quo (see also refs. 2 and 3), resulting in suboptimal decision making. Using a model of effective connectivity inspired by computational models of action selection (9, 10), we provide evidence that IFC increases its influence on the STN when a difficult default is rejected. Our task was intended to elucidate the mechanisms involved in overcoming a status quo bias for simple perceptual decisions requiring overt actions, and we are cautious in extrapolating the mechanisms underlying a similar bias for more complex cognitive or value-based decisions. However, taken together, our results suggest that rejection of the status quo during difficult decisions invokes specific neural dynamics within prefrontal–basal ganglia circuitry. At a broader level such mechanisms may contribute to rejecting the default in scenarios ranging from retirement fund decisions to consumer choice.

Methods

Participants. Seventeen healthy right-handed subjects who provided informed consent took part in the study. All had normal or corrected-to-normal vision and no history of psychological or neurologic illness. One participant was excluded because of poor behavioral performance (33% errors on low-difficulty trials). Sixteen subjects' data were analyzed (5 male; 19–34 years of age; mean age, 25.3 years). The study was approved by the Institute of Neurology (University College London) Research Ethics Committee. Participants received a fixed reimbursement plus a small bonus payment calculated from their best-scoring block of trials.

Task and Procedure. Each trial began with a central fixation cross flanked by two longitudinal white tram lines presented in peripheral vision. Participants were asked to maintain fixation and were instructed that not doing so would compromise their performance on the line judgment task. The target ball was presented at either tramline either overlapping the line (in) or outside the line (out). The difficulty of the decision was manipulated by altering the distance of the stimulus from the outside edge of the tramline. Responses were made using an optical keypad and consisted of a go/no-go decision to reject or accept the default, respectively. See Fig. 1 legend and *SI Text* for further details.

Behavioral Analysis. Behavioral responses were classified according to whether the trial led to a rejection or acceptance of the default, and whether the trial was high or low difficulty. A status quo bias was assessed by comparing the proportion of trials leading to an acceptance response on high- and low-difficulty trials, using a two-tailed paired *t* test. Each participant's decision criteria (c) and sensitivity (d') were estimated from the data using signal detection theory (SDT; see Fig. 1*B*), whereby the hit rate (H) was defined as p("in"|ball = in) and false alarm rate (F) as p("in"|ball = out). Decision criteria and d' for each difficulty level (high/low, indexed by i) and default position (in/out, indexed by j) can then be calculated as follows (40), where z is the inverse of the normal distribution function:

$$c_{ij} = -0.5\left[z(H) + z(F)\right]$$

$$d'_{ij} = z(H) - z(F)$$

SDT parameters and error rates were analyzed using repeated-measures ANOVA.

fMRI Analysis. We acquired brain data using a 3T Allegra scanner (Siemens). See *SI Text* for details of image acquisition and preprocessing. Functional data were analyzed using SPM5 (www.fil.ion.ucl.ac.uk/spm). Stimulus onsets were separated into two regressors depending on the perceptual difficulty on each trial (high/low). Choice screen onsets were separated into six regressors dependent on whether the trial was high/low difficulty, whether it led to an accept/reject response, and, on high-difficulty trials, whether this response was correct or incorrect (*reject_high_correct*, *reject_high_incorrect*, *reject_low*, *accept_high_correct*, *accept_high_incorrect*, *accept_low*). Response accuracy (correct/incorrect) was not modeled as a separate factor on low-difficulty trials, given the relative rarity of incorrect responses (4.9% ± 1.0%, SEM). The *reject* stick functions were parametrically modulated by the reaction time on each trial, and the cumulative feedback stick function was modulated by the amount of money won on the previous 10 trials. Our critical contrast of interest (the interaction of default rejection and difficulty, collapsing across correct/incorrect) was computed as follows: [*reject_high_correct* = +0.5; *reject_high_incorrect* = +0.5; *reject_low* = −1; *accept_high_correct* = −0.5; *accept_high_incorrect* = −0.5; *accept_low* = +1].

Cluster-based statistics were used to define significant activations both on their intensity and spatial extent (41). Clusters were defined using a threshold of $P < 0.005$ and corrected for multiple comparisons within a given search volume using FWE correction and a threshold of $P < 0.05$. SVC was applied to a priori ROIs in the STN and MFC. See *SI Text* for further details.

Connectivity Analysis. We conducted DCM analysis using SPM8 (www.fil.ion.ucl.ac.uk/spm). DCM models neural dynamics in a system of interacting brain regions by representing the population activity at the neural level with a single state variable for each region (25); see *SI Text* for further details. We constructed nine DCMs covering the three combinations of default rejection affecting the flow of information from frontal cortex to STN, crossed with three possible architectures for how decision difficulty affects the network. Specifically, *difficulty* either drove rIFC, MFC, or both; *reject* either modulated rIFC to STN, MFC to STN, or both. In all nine models each of the three areas was reciprocally connected, according to known anatomic connectivity in humans and macaques (12, 13). See *SI Text* for details of time series selection. These models were compared at the group level using a random-effects procedure implemented in SPM8 (42). Once the best model was established, we determined which set of connections was consistently affected by default rejection across subjects. This was realized by applying classical statistics at the second level to the maximum a posteriori estimates of the parameters from individual subject DCMs, using a two-tailed *t* test against zero.

ACKNOWLEDGMENTS. We thank P. Haggard, S. Bestmann, and T. Sharot for insightful comments on earlier versions of the manuscript. This work was carried out under a Wellcome Trust Programme Grant (to R.J.D.) and Medical Research Council funding within the University College London 4-Year Ph.D. in Neuroscience (to S.M.F.).

1. Samuelson W, Zeckhauser R (1988) Status quo bias in decision making. *J Risk Uncertain* 1:7–59.
2. Dhar R (1997) Consumer preference for a no-choice option. *J Consum Res* 24:215–231.
3. Iyengar SS, Lepper MR (2000) When choice is demotivating: Can one desire too much of a good thing? *J Pers Soc Psychol* 79:995–1006.
4. Limousin P, Martinez-Torres I (2008) Deep brain stimulation for Parkinson's disease. *Neurotherapeutics* 5:309–319.
5. Bergman H, Wichmann T, DeLong MR (1990) Reversal of experimental parkinsonism by lesions of the subthalamic nucleus. *Science* 249:1436–1438.
6. Frank MJ, Samanta J, Moustafa AA, Sherman SJ (2007) Hold your horses: Impulsivity, deep brain stimulation, and medication in parkinsonism. *Science* 318:1309–1312.
7. Hershey T, et al. (2004) Stimulation of STN impairs aspects of cognitive control in PD. *Neurology* 62:1110–1114.
8. Alberts JL, et al. (2008) Bilateral subthalamic stimulation impairs cognitive-motor performance in Parkinson's disease patients. *Brain* 131:3348–3360.
9. Frank MJ (2006) Hold your horses: A dynamic computational role for the subthalamic nucleus in decision making. *Neural Netw* 19:1120–1136.
10. Gurney K, Prescott TJ, Redgrave P (2001) A computational model of action selection in the basal ganglia. I. A new functional anatomy. *Biol Cybern* 84:401–410.
11. Aron AR, Poldrack RA (2006) Cortical and subcortical contributions to Stop signal response inhibition: Role of the subthalamic nucleus. *J Neurosci* 26:2424–2433.
12. Nambu A, et al. (2000) Excitatory cortical inputs to pallidal neurons via the subthalamic nucleus in the monkey. *J Neurophysiol* 84:289–300.
13. Aron AR, Behrens TE, Smith S, Frank MJ, Poldrack RA (2007) Triangulating a cognitive control network using diffusion-weighted magnetic resonance imaging (MRI) and functional MRI. *J Neurosci* 27:3743–3752.
14. Aron AR, et al. (2007) Converging evidence for a fronto-basal-ganglia network for inhibitory control of action and cognition. *J Neurosci* 27:11860–11864.
15. Isoda M, Hikosaka O (2007) Switching from automatic to controlled action by monkey medial frontal cortex. *Nat Neurosci* 10:240–248.
16. Isoda M, Hikosaka O (2008) Role for subthalamic nucleus neurons in switching from automatic to controlled eye movement. *J Neurosci* 28:7209–7218.
17. Mather G (2008) Perceptual uncertainty and line-call challenges in professional tennis. *Proc Biol Sci* 275:1645–1651.
18. Basso MA, Wurtz RH (1997) Modulation of neuronal activity by target uncertainty. *Nature* 389:66–69.
19. Johnson EJ, Goldstein D (2003) Medicine. Do defaults save lives? *Science* 302: 1338–1339.
20. De Martino B, Kumaran D, Holt B, Dolan RJ (2009) The neurobiology of reference-dependent value computation. *J Neurosci* 29:3833–3842.
21. Kahneman D, Knetsch JL, Thaler RH (1991) Anomalies: The endowment effect, loss aversion and status quo bias. *J Econ Perspect* 5:193–206.
22. Anderson CJ (2003) The psychology of doing nothing: Forms of decision avoidance result from reason and emotion. *Psychol Bull* 129:139–167.
23. Botvinick MM (2007) Conflict monitoring and decision making: Reconciling two perspectives on anterior cingulate function. *Cogn Affect Behav Neurosci* 7:356–366.
24. Stephan KE, et al. (2007) Dynamic causal models of neural system dynamics: Current state and future extensions. *J Biosci* 32:129–144.
25. Friston KJ, Harrison L, Penny W (2003) Dynamic causal modelling. *Neuroimage* 19: 1273–1302.
26. Thaler RH, Sunstein CR (2008) *Nudge: Improving Decisions About Health, Wealth and Happiness* (Yale Univ Press, New Haven, CT).
27. Ray NJ, et al. (2009) The role of the subthalamic nucleus in response inhibition: Evidence from deep brain stimulation for Parkinson's disease. *Neuropsychologia* 47: 2828–2834.
28. van den Wildenberg WP, et al. (2006) Stimulation of the subthalamic region facilitates the selection and inhibition of motor responses in Parkinson's disease. *J Cogn Neurosci* 18:626–636.
29. Baunez C, et al. (2001) Effects of STN lesions on simple vs choice reaction time tasks in the rat: Preserved motor readiness, but impaired response selection. *Eur J Neurosci* 13: 1609–1616.
30. Eagle DM, et al. (2008) Stop-signal reaction-time task performance: Role of prefrontal cortex and subthalamic nucleus. *Cereb Cortex* 18:178–188.
31. Cohen MS, et al. (2008) Deep brain stimulation to the subthalamic nucleus modulates conflict processing and cortical oscillatory dynamics in Parkinson's patients. *Soc Neurosci Abs* 682.17. Available at www.sfn.org.
32. Lalo E, et al. (2008) Patterns of bidirectional communication between cortex and basal ganglia during movement in patients with Parkinson disease. *J Neurosci* 28: 3008–3016.
33. Mars RB, et al. (2009) Short-latency influence of medial frontal cortex on primary motor cortex during action selection under conflict. *J Neurosci* 29:6926–6931.
34. Buch ER, Mars RB, Boorman ED, Rushworth MFS (2010) A network centered on ventral premotor cortex exerts both facilitatory and inhibitory control over primary motor cortex during action reprogramming. *J Neurosci* 30:1395–1401.
35. Li CSR, Yan P, Sinha R, Lee TW (2008) Subcortical processes of motor response inhibition during a stop signal task. *Neuroimage* 41:1352–1363.
36. Xue G, Aron AR, Poldrack RA (2008) Common neural substrates for inhibition of spoken and manual responses. *Cereb Cortex* 18:1923–1932.
37. Chambers CD, et al. (2006) Executive "brake failure" following deactivation of human frontal lobe. *J Cogn Neurosci* 18:444–455.
38. Clark L, et al. (2007) Association between response inhibition and working memory in adult ADHD: A link to right frontal cortex pathology? *Biol Psychiatry* 61:1395–1401.
39. Mostofsky SH, Simmonds DJ (2008) Response inhibition and response selection: Two sides of the same coin. *J Cogn Neurosci* 20:751–761.
40. Macmillan NA, Creelman CD (2005) *Detection Theory: A User's Guide* (Lawrence Erlbaum, New York).
41. Friston K, Worsley K, Frackowiak R, Mazziotta J, Evans A (1994) Assessing the significance of focal activations using their spatial extent. *Hum Brain Mapp* 1: 214–220.
42. Stephan KE, Penny WD, Daunizeau J, Moran RJ, Friston KJ (2009) Bayesian model selection for group studies. *Neuroimage* 46:1004–1017.